ULTRAVIOLET LIGHT GENERATION FROM A HELIUM PLASMA AS A FUNCTION OF RADIO FREQUENCY POWER AND GAS PRESSURE

A Thesis

in Partial Fulfilment of the Requirements for the

Degree of Master of Science

With a

Major in Physics

in the

College of Graduate Studies

University of Idaho

by

Ahmed Alanazi

Major Professor: David N. McIlroy, PhD.
Committee Members: Jason W. Barnes, PhD., Matthew M. Hedman, Ph.D.
Department Chair: Ray Von Wandruszka, Ph.D.

August 2017

Authorization to Submit Thesis

The thesis of Ahmed Alanazi, submitted for the degree of Master of Science with a major in Physics and titled, "ULTRAVIOLET LIGHT GENERATION FROM A HELIUM PLASMA AS A FUNCTION OF RADIO FREQUENCY POWER AND GAS PRESSURE," has been reviewed in final form. Permission, as indicated by the signatures and dates given below, is now granted to submit final copies to the College of Graduate Studies for approval.

Major Professor: _____ Date: _____

David N. McIlroy, Ph.D.

Committee Members: _____ Date: _____

Jason W. Barnes, Ph.D.

_____ Date: _____

Matthew M. Hedman, Ph.D.

Department Chair: _____ Date: _____

Ray Von Wandruszka, Ph.D.

Abstract

Ultraviolet (UV) light emission is generated by exciting ground state helium to excited states, where the characteristic UV emission lines are referred to as the helium I and helium II emission lines. Excited He is achieved by pumping He gas with electromagnetic (EM) energy, where both ionized and excited He co-exist, known as a He gas plasma. The intensity UV emission by the He plasma increases with EM pumping power and the He gas pressure. Consequently, He plasmas are used as UV light sources. The highest intensity He UV light sources incorporate electron cyclotron resonance (ECR), where ECR increases the light intensity by increasing the probability of collision between the free electrons in the plasma with the He atoms. This class of high intensity UV light sources exclusively us microwaves to generate the He plasma. To the best of our knowledge, no one has attempted to use radio frequency (RF) EM radiation in high intensity UV light sources. Why not? RF plasmas are much easier to generate and control. All that is required is a simple electronic matching network for tuning the plasma, while a microwave plasma requires an antenna and a resonance chamber for tuning. In the present study, a high intensity He UV light source has been constructed using a ECR enhanced RF He plasma. Due to the absorption of low energy UV light by air, the emission and energy of the UV source has been indirectly measured by monitoring the photoelectron current of a gold target placed in the beam of the light source and rationalized by comparing to spectroscopy data reported for He plasmas. At low gas pressure the profile of the photocurrent consists of two pair of maxima. The pair of maxima in the low He gas pressure regime are assigned to the helium II emission lines with photon energies of 40.8 eV and 48.3 eV, respectively. In the high He pressure regime the pair of maxima are assigned to helium I emission lines at photon energies of 21.2 eV and 23.1 eV, respectively. Photocurrents of the order of a few pA have been obtained, as opposed to tens of nA for a traditional DC He UV light source.

Acknowledgments

I would like to thank all the people who contributed in some way to the work described in this thesis. First and foremost, I thank my academic advisor, Professor David N. McIlroy, for accepting me into his group. Additionally, I would like to thank Dr. Jason W. Barnes, and Dr. Matthew M. Hedman for being on my committee. Also a big thanks to Nathan Dice and Marshall Boyland for their help in the laboratory.

Dedication

To my parents and my wife for their invaluable support since I started school. To my family and friends for the encouragement they gave me to finish this degree.

Table of Contents

List of Figures

List of Tables

CHAPTER 1: Introduction

Gas discharge lamps have been used as light sources in photoelectron spectroscopy [14]. Most commonly, helium discharge lamps are one of the most common light sources that are excited by DC discharge or by radio frequency power discharge in the presence of helium gas [14]. Various pressures of helium for the gas discharge are used to generate light at different energies. The characteristics of helium sources provided by Samson and others for ultraviolet photoelectron spectroscopy are: (i) DC cold-cathode discharge [6], (ii) Microwave discharge [13], (iii) condensed spark [6], (iv) and the duoplasmatron [6]. Due to the excitation by DC discharge or AC discharge, helium discharge lamps produce resonance emission lines at photon energies of 21.2 eV (He I-) and 40.8 eV (He II-) [6,14-15]. Also, helium discharge lamps provide other resonance emission lines at photon energies of 23.1 eV (He I-) and 48.3 eV (He II-) [6,14-17]. The atomic lines are due to the electronic transition in excited helium atoms [6]. The new generation of discharge lamps use the Electron Cyclotron Resonance (ECR) technique to create helium plasma at low pressure. The ECR technique induces a circular trajectory of the electrons, which increases the probability of interaction of the helium molecules with electrons, thereby generating a higher intensity ultraviolet radiation [16]. Among the different types of UV light sources, we have investigated the use of radio frequency (RF) power to excite helium atoms and indirectly evaluated the emission of the helium resonance lines at low and high pressure, where the literature has shown that the atomic emission lines of helium is pressure dependent [6,14-19]. It was shown that operating the helium lamp at high pressure produces the (He I) light at photon energies 21.2 eV and 23.1 eV, while operating at low pressure produces the (He II) light at photon energies 40.8 eV and 48.3 eV [6,14-17]. In this chapter, we will provide a review of the plasma state, such as plasma formation, temperature, Debye or plasma parameter, degree of ionization, energy level, collision theory and probability in a plasma, quantum number and electron configuration, and about ECR.

1.1. What is a plasma and how is plasma made?

By definition, a plasma is an ionized gas [20]. It is often referred to as a a fourth state of matter in the following sequence: solid, liquid, gas and plasma [9]. When applying high temperature to a solid material, the thermal motion of the atoms breaks the lattice bonds,

resulting in a liquid state. When increasing the temperature of the liquid, the atoms or molecules vaporize to form a gas state. By further raising the temperature of the gas the atoms are ionized ergo; a plasma is formed [20]. In other words, a plasma contains electrons, positive ions and neutral particles. The neutral particles and ions are the heavy particles of the plasma state [9]. The plasma has physical characteristics associated with the dynamic motion of the ions, neutrals and electrons. The electric field in the plasma depends on the charge separation between local concentrations of the ions and electrons. Because the charged particles are constantly in motion, they produce currents and accompanying magnetic fields [20]. The plasma is quasi-neutral, indicating that the ion density and electron density are almost equal [9]. The most straightforward way to generate a plasma is with a DC electric field that is strong enough to ionize the gas. However, this approach doesn't produce a sufficient quantity of ions and the unidirectional electric field doesn't favor a large ion/electron density. In an ideal plasma the electric field provides energy to free electrons, which in turn collide and ionize the atoms of the gas, thereby liberating more electrons [20]. In essence, a cascading ionization of the gas occurs if the gas pressure is sufficiently high and sufficient energy is pumped into the system.

1.2. Debye Shielding and Plasma Parameter

Considering a positive charge (ion) in a plasma, an electron cloud is attracted to the ion due to their mutual Coulombic attraction. The cloud of free electrons surrounding the positive ion screen it from other electrons in the plasma and neighboring ions. One can consider the ion-electron cloud to be a spherical unit cell, so to speak, of the plasma. By definition, the radius of the spherical unit cell is the point at which the electric field of the ion is completely shielded by the electron cloud. This characteristic length of the plasma is called the Debye length and the shielding is known as Debye shielding. The Debye shielding reduces the repulsion force between the ions. The Debye length is a function of particle density and the plasma temperature. The Debye length increases with plasma temperature but decreases with particle density. Increasing the temperature of the plasma causes it to expand and subsequently the Debye length increases. Without a plasma pressure, the cloud of electrons around the ions tend to collapse to a very small volume. The Debye length or Debye radius is the fundamental dimension used to describe the plasma. To create a plasma, the

electron density must be large enough such that the Debye radius is shorter than the dimension of the plasma system [21].

1.3. Temperature in Plasma

The plasma is defined by its density, pressure and temperature. It is meaningless to define the temperature or pressure of a single particle in a plasma, however, the temperature and pressure of an ensemble of particles is very is a useful approach for describing the plasma, i.e. the plasma can be accurately describe with statistical mechanics. This is because the particles are moving with different speeds. Note, the electrons collide with ions and other electrons. In the collision process, the electrons can gain or lose energy. The temperature is related to the kinetic energy of the particles in the plasma. The particles in a hotter plasma wider range of kinetic energy [21]. The plasma temperature is given in units of energy (eV). The energy corresponding to K_BT and is used to define the plasma temperature. For example, when referring to a 41eV plasma, it means that K_BT = 41 eV, or a plasma temperature of T= 473465 K, or an average energy of E=3/2 K_BT = 61 eV [22]. In other words, the plasma temperature is the average kinetic energy of a particle [9]. When the gas pressure in the chamber is increased, the collisions between the electrons and gas atoms increases, which increase in the gas temperature at the expense of the electron temperature. Finally, power pumped into the plasma increases the electron density and electron temperature in the chamber due to the secondary electrons emitted from the power input electrodes, further enhancing the probability of ionizing events [23].

1.4. Degree of Ionization of a Plasma

To form a plasma, ionization of the gas is necessary, where ionization is the process whereby an atom absorbs energy and a free electron is emitted, leaving positively charged ion. The degree of ionization depends on the average energy of free electrons. However, there is a measure of conditions where only a fraction of the atoms are ionized [20]. In a high temperature plasma the degree of ionization is high due to collisions with other charged particles. Conversely, at low temperatures the degree of ionization is low due to collisions between neutral particles and charged particles [20].

1.5. Energy Level Transition

The structure of an atom contains one or more electrons bound to the nucleus [8]. The transition of an electron from one quantum state to another within an atom is associated with the emittance or absorption of electromagnetic radiation. In this case, a photon energy must be equal to the energy difference between the ground state level and excited state level, where the lowest energy level of the atom is the ground state, while any state of the atom above the ground state is an excited state [9]. An atomic transition can be described by three types of transitions. Stimulated absorption, in which an absorption of a photon transitions the atom to a higher energy level; spontaneous emission, in which the atom emits a photon and transitions from an excited state to a lower state; and stimulated emission, where the incoming photon de-excites the atom, which subsequently emits a photon similar to the incoming photon [1].

1.6. Collision Theory in a Plasma

Different phenomena take place when two particles collide. If there are no changes in the internal energies of collision, then the total of kinetic energy is conserved and the collision is called **elastic**. If the internal energies of the collision are changed, then the total kinetic energy is not conserved and the collision is called **inelastic** [8]. For instance, the particles may vary their energy or momentum, neutral atoms may become ionized, and ionized atoms may become neutral [8,9]. The main processes of collisions of the electrons with atoms are elastic collisions in which the momentum of the electron is changed, and inelastic collision in which excitation and ionization take place. For the collisions of ions with atoms, the collision is elastic with energy and momentum exchanged and resonant charge transfer occurs. The collision conserves the energy and momentum only when the energy and the total momentum are equal to each other before and after the collision. In the case of a ionizing event the electrons are free and are defined by their kinetic energy. For partially stripped ions, i.e. the electrons are still bond but at in a very high bound state, they can be further excited and ionized. The sum of the potential and kinetic energy is the total energy and conserved in a collision.

The excitation process occurs when an atom or molecule absorbs the incoming light, and the energy of the incoming light is equal or higher than the energy difference between the ground state and the upper state. It also may occur when an atom collides with an electron or a

heavy particle causing a bound electron to escape from the ground state to a higher energy level. In contrast, the ionization process may occur when an atom or molecule removes an outer electron by absorbing sufficient energy during a collision with an electron or heavy particle or through absorption of a photon [9].

1.7. Collision Probability

The probability of a particle colliding with another particle in a medium relies on three factors: the density of gas, the mean free path, and cross section. The mean free path is the average distance between particles before they experience a collision. It is inversely proportional to the gas density in the medium, which indicates that the mean free path depends on the gas density and the effective scattering cross section [21]. When the gas density is high, the mean free path becomes short, because the particles are very close to one another, and the probability of a collision is high [21, 24]. When the gas density is low, the mean free path becomes long, and the probability of a collision is low [21, 24].

The collision cross section is the theoretical area of contact between particles that describes the scattering event. Specifically, it is the total effective area. The contact area varies for each type of collision. For example, the effective area is larger for an ionization event than for an excitation event. The total effective cross section is the sum of the specific cross section for specific types of collision. If q_1,q_2,q_3 … etc., are the cross sections for ionization, excitation, charge transfer, etc., respectively, then the total effective of cross section is as the following [25]:

$Q= q_1+q_2+q_3+...$

The collision cross section depends on the relative velocity between of the collision. For a Coulombic interaction, increasing the relative velocity between the particles decreases the total effective cross section because the probability of deflection is small [21].

Another characteristic of a collision in a plasma is the collision frequency or rate of collisions. It is is the number of collisions per unit time for a given system. The collision frequency depends on three quantities; gas density, cross section and the velocity of the particles. In the collision process, the cross section decreases with increasing velocity of the particle, causing a decrease of the collision frequency. In addition, raising the temperature causes the collision frequency to decrease. For extremely high temperature in a plasma, the

collision frequency becomes very small until the plasma effectively becomes collision-less. Also, the collision frequency is inversely proportional to the mean free path, i.e. for lower collisions frequency the mean free path becomes longer [21].

1.8. Quantum Number and Electron Configuration

In the quantum theory of atoms, the energy of an electron and its location is described in terms of probability. In an atom, electrons do not exist in individual orbitals but rather they occupy a region of space around the nucleus. The probability of finding an electron with a specific energy and momentum in the atom is the electron's quantum numbers. In other words, the quantum numbers tell us about the address of an electron in the orbitals. The quantum numbers of all the electrons of an atom is referred to as the atom's electron configuration.

To describe the electron in an atom, it is very important to consider the following quantum numbers [26]. The principle quantum numbers are characterized by the letter n. It describes the electrons shell and is an integer number starting from 1. The principal quantum numbers tell us how far the orbital is from the nucleus. It also explains the energy level that the electrons occupy around the nucleus. The electrons in the same orbital surrounding the nucleus have the same electron shell and principle quantum number [26]: n= 1,2,3,4,5,6 and main shell = K,L,M,N,O,P. The angular momentum quantum numbers are characterized by the letter l. It describes the shape or symmetry of a specific orbital shape. The angular momentum quantum number depends on the principle quantum number and ranges from 0 to n-1. The subshell letters are used to describe l values [26]: l values 0,1,2,3,4 and subshell s,p,d,f,g.

The magnetic quantum numbers are characterized by the letter m_l. It tells us the orientation of the orbital in space. The magnetic quantum numbers of m_l can range from -1 to +1, including 0. For example, when l=0, then m_l can only be 0, and when l=1, ml can have the following values -1, 0,+1 [26]. The spin quantum numbers are characterized by the letter m_s. It describes the electron spin, which can either be spin up (1/2) or spin down (-1/2) [26].

The electron configuration describes the distribution of electrons in an atom's orbitals starting from the lowest energy level to the highest energy level. For example, the electron

configuration of a hydrogen atom is $1s^1$. The initial number 1 indicates that the electron contains a principle quantum number of n=1 and is in the main shell K. The s indicates that the electron has an l = 0 and occupies s-orbital. The subscript 1 means that the orbital has one electron of a possible two. Another important aspect is the Aufbau principle, which originates from the Pauli principle exclusion. It states that no two electrons have the same four quantum numbers. The occupation of orbitals in an atom with electrons has to build up from lower to higher energy levels. They occupy orbitals in order of increasing energy. The maximum electron occupancy for the orbitals s,p,d,f, are 2,6,10,14, respectively. The expression of the electrons' occupation is as the following [26]:

1s<2s<2p<3s<3p<4s<3d<4p<5s<4d<5p<6s<4f<5d<6p<7s<5f<6d<7p

1.9. Electron Cyclotron Resonance (ECR)

Consider a charged particle moving with velocity in the presence of a magnetic field and electric field. The particle experiences a force due to the electric field and another due to the magnetic field. This is the Lorentz Force. The magnetic force is perpendicular to the plane containing the velocity and magnetic field vectors. The magnetic force acts to create centripetal acceleration, which causes a charged particle to move in a circular motion or cyclotron motion [1]. In the vernacular of plasmas, a system where electrons exhibit cyclotron motion is electron cyclotron resonance or ECR. In the context of a plasma, cyclotron motion increases the probability of collisions, thereby, increasing the probability of an atom in the plasma being excited and the subsequent emission of ultraviolet radiation. Utilizing ECR in a UV discharge lamp enables a plasma a lower pressure than one without ECR. The frequency of the AC power used to create the plasma must be synchronized with the ECR frequency in order to confine the electrons within the volume of the plasma. Thus, when the mobile electrons interact with the gas in the chamber they ionize the gas if their kinetic energy is higher than the ionization energy of the atoms or molecules. Once the ions are produced, the ECR is able to confine the electrons in order to maintain collision and ionization for a long time [16,8].

The placement of the four magnets creates a magnetic field that from the reference frame of the electron changes its direction as the electron propagates forward. As the electric and magnetic fields become misaligned the varying electric field will pump energy into the

electron and it will move on a spiral trajectory, increasing its velocity $v_\perp$ and hence the gyration radius. The trajectory is described by the following figure:

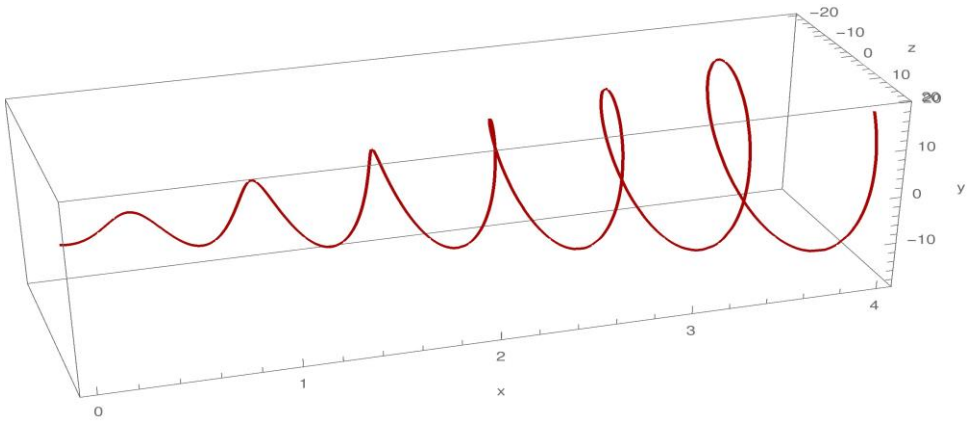

Figure 1.1 Electron Trajectory

In the figure the *x* axis is aligned with the magnetic field, and the electric field now has a component which varies in the *x*-*z* plane.

The time-varying electromagnetic field has a negligible effect on the trajectory at first. However, as the helix continues to wind around the magnetic field line and the field line starts to turn due to the placement of the magnets, the component of the electric field perpendicular to the magnetic field gets into a resonance with the motion of the electron and start to dump energy into it. Consequently, the electron increases its velocity and the radius of the helix, since $r \propto v_\perp$ [27].

CHAPTER 2: Theoretical Approach

2.1. The Theory of Photoelectric Effect

The photoelectric effect is the phenomenon that led to a quantum model of light. In 1887, the story of photoelectric effects starts with Hertz, when he worked on the confirmation of Maxwell's electromagnetic wave model of light. Hertz showed that the speed of electromagnetic wave is equal to the speed of light. He noticed that when ultraviolet radiation strikes a cathode surface, a charged particle loses its charge more rapidly due to ultraviolet radiation [1-4]. In 1888, Hallwachs investigated this phenomenon, and he found that in a zinc plate, the negatively charged plate emits a negative charge when illuminated by ultraviolet radiation, while there is no effect on the positively charged plate. In 1899, J.J. Thomson's charge-to-mass ratio experiment proved that the negative particles emitted from a cathode are electrons due to the ultraviolet light [2]. In 1900, Philip Lenard showed that when light is incident on a metal surface, electrons are ejected. When these electrons arrive to the anode (collector), a current value appear in the external ammeter. Lenard noticed that the highest value of current was proportional to the radiation intensity, since doubling the amount of energy per unit time incident on the emitter should double the amount of particles emitted. At low Intensities, there are no emission particles produced to escape from the metal [3]. The data collected by Lenard was not enough to give a full explanation of the photoelectric effect [5].

If one applies the classical electromagnetic wave theory of light to the photoelectric effect, it predicts that the ejection of photoelectrons isn't instantaneous because the electron in the material must absorb enough electromagnetic energy, which takes time. The classical electromagnetic model states that the amount of energy in the radiation wave increases as the light intensity increases and therefore should causes photoelectrons to emitted sooner than with low intensity light. Consequently, as the light intensity is increases, the time required to observe photoelectrons is shorter and the photoelectrons will have more kinetic energy, and absorb the energy continuously from the radiation, i.e. accelerate. In addition, there should be a time interval between the incident radiation and the ejection process of photoelectrons. At very low radiation intensities, a significant time delay should be observed between turning on the light and observing a photocurrent, where the time is needed for the electrons to absorb

sufficient radiation to overcome the work function of the metal. Photoelectrons should be emitted from the surface of a material at any incident radiation frequency, as long as the radiation intensity is high enough, because the energy of light is delivered to the metal regardless of the incident radiation frequency, i.e. the frequency of the radiation and the electron kinetic energy are unrelated. Instead, the kinetic energy of electrons should be a function of the intensity of the radiation.

On the other hand, for high intensity radiation the photocurrent should be a maximum, again independent of the light frequency. Basically, more electrons are removed from the metallic surface by the higher-intensity light.

Unfortunately, the experimental results of the photoelectric effect do not agree with the aforementioned classical model. First, the experimental time delay between turning on the light and the photoemission of electrons is less than 10^{-9} s, which is essentially instantaneous and therefore contradicts the predictions of the classical model. Further experimental studies of the photoelectric effect reveal other discrepancies. When the electric potential (ΔV) between the two plates (emitter and collector) of the experimental setup is negative, i.e. the power supply is reversed to make the emitter positive and the collector negative, thereby creating a retarding potential, the current decreases because the emitted electrons (photoelectrons) from the positive plate are repelled by the negative plate (collector). Under these conditions, only photoelectrons that have a kinetic energy larger than $e|\Delta V|$ reach the collector, where e is the value of the charge on the electron. When the retarding potential is equal or more negative than the kinetic energy of the photoelectrons, no photoelectrons reach the collector and the current is zero. Furthermore, the retarding potential (stopping potential) that stops all photoelectrons from reaching the collector is frequency dependent. Correspondingly, the maximum kinetic energy of the photoelectrons depends on the frequency of light. In addition, no photoelectron emission occurs when the incident radiation frequency drops below a specific threshold frequency, regardless of the radiation intensity and the maximum kinetic energy of the photoelectrons increases with increasing radiation frequency. The existence of minimum light frequency that produces photoelectrons is attributed to the presence of a potential energy barrier specific to the metal, referred to as the work function ϕ of the metal, which all photoelectrons must overcome. The work function explains why grounded metals do not spontaneous conduct electricity or emit electrons. If the

energy of the arriving light is not greater than the work function barrier (ϕ), then no photoelectrons are produced. The photons with lower frequency than the cutoff frequency for a given metal do not have enough energy to excite the electrons across the work function barrier. The scientific community arrived at the conclusion that the accepted wave nature of electromagnetic radiation (light) was incompatible with the photoelectric effect experiments and no one had an explanation.

In 1905, Einstein proposed that light could act either as an electromagnetic wave or as a particle, known as a photon. In Einstein's particle model of light (photon), the photon has a fixed quantity of energy *hf*, where h is Planck's constant and f is the frequency of the photon. Consequently, the photon can deliver all of its energy instantaneously. In this case, the absorption process of energy via the electrons is a discontinuous process, which means that the energy transfer to the electrons in the discrete bundles. This eliminates the need for the electron to wait to absorb sufficient light to overcome the work function barrier. The energy transport is by a one photon-one electron event. According to Einstein, the photoelectric effect equation is given by [1-4]:

$$K = hf - \phi,$$

where K is the kinetic energy of the photoelectron, ϕ is the work function, the barrier that keeps electrons from spontaneously being ejected from the metal. It sets the limit on the lowest binding energy of the electrons to the metal [4]. If the light intensity is increased, the number of photons that transfer per unit time increases, thereby increasing the number of photoelectrons ejected. Einstein's model resolves all of the issues associated with the application of the classical electromagnetic theory of light to the photoelectric effect. The rest is history.

2.2 The Glow Discharge

The backbone of a plasma discharge is a voltage source that provides power between two electrodes (cathode and anode) in the presence of the gas that is to be ionized. Note, there are some regions between the cathode and the anode regions that will be involved in generating plasma ignition. The general description for the geometry of the glow discharge is that a glow discharge contains two regions known as light and dark regions. The geometry of DC glow discharge starts from the cathode region, which is the Aston dark space. Next to the

cathode region is the glow area known as the cathode glow. Next to the cathode glow is another dark region known as the cathode dark space or the Crookes dark space. Also next to the cathode dark space is the negative glow that encompasses a larger volume and is more intense than the cathode glow. This is followed by the Faraday dark space, which is next to the negative glow region. Next to the Faraday region, there is the positive column, which occupies the entire remaining region of the discharge [6].

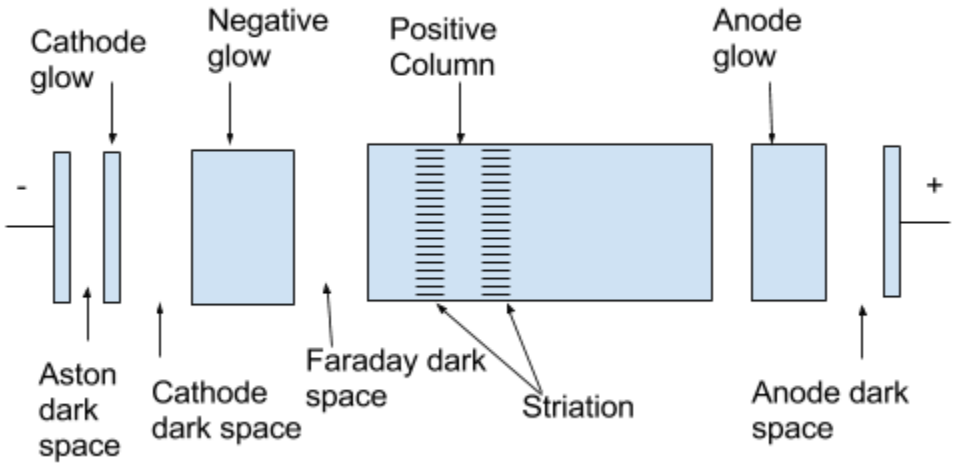

Figure 2.1 A schematic of the regions in a DC glow discharge

In the positive column, the striation phenomenon depends on the gas pressure, gap distance and the discharge current [7]. Following this is the anode glow. Finally, towards the anode there is the region called the anode dark space. The specifics of these regions of the plasma depend on the type of gas, pressure and voltage. Under specific conditions, the positive column and anode glow could disappear, but the characteristics at the cathode region are likely permanent with the maintenance of the discharge [6].

The role of the electric field between the electrodes is to generate electrons that excite neutral atoms and ions. The excitation process takes place in the negative glow region. Since the electrons are accelerated toward the Faraday dark space, the potential drop between the electrodes becomes very low and therefore the electrons will not have enough energy to generate ionic species in the positive column region. Thus, in general, neutral atoms are excited in the positive column region and, therefore, radiation originates from the positive

column region. Conversely, the glow discharge from the negative glow region is due to the excitation of ions and atoms [6].

In the negative glow region, the magnitude of the potential drop between the electrodes determines the degree of excitation. In addition, the potential drop depends on the type of gas and electrode material. The potential drop increases with the work function of the cathode material. This means that the cathode drop goes up further with current since the discharge is applied in the abnormal glow region [6].

In the case of the glow discharge, only a part of the cathode behaves like an emitter. The current density in the cathode becomes constant as the discharge current goes up; however, in this case, the size of the cathode surface is involved and the cathode drop becomes constant. When the discharge current goes up, the transition between the normal glow and the abnormal glow will take place, and therefore the cathode drop is occupied by the negative glow region and the entire surface of the cathode drop will behave like an emitter. The consequence of increasing the discharge current is that the cathode current density will increase, as well as the potential drop in the cathode area. In general, if it is required to acquire the normal glow with high discharge current, the surface of the cathode is best to be as large as possible. In contrast, if it is required to generate high cathode drop, the abnormal glow should be involved. To approach this condition in the low magnitude of the discharge current, the cathode surface should be small in the small area. Normally, the intensity of radiation increases with discharge current and the portion size of the cathode surface region is responsible for producing the highest discharge current without causing a transition to the arc discharge region. In short, as long as the cathode surface is large, the maximum discharge current is achieved. To achieve high intensity of the radiation from the glow discharge region, it is required to keep and confine the discharge in a capillary with a specific length, usually between 10 to 20 cm and with a hole between 3 to 5 mm. This condition will increase the intensity of light and make it possible to see the discharge along the axis of the capillary. The positive column region will cover and fill the whole length of the capillary and is the source of the light that is observed [6].

2.3 AC Discharge

Alternating current (AC) power also is suitable for generating a gas plasma. In fact, AC plasmas are much more common than DC plasmas. The advantage of AC power is that one can generate plasmas using different ranges of frequencies. Frequency is another tool in one's plasma toolbox for optimizing a plasma. The most common frequency range for generating a plasma is the radio frequency (RF). Radio frequency discharge is used to excite electrodeless ring discharge and linear discharge to generate vacuum ultraviolet radiation. The spectrum generated by the RF is similar to that produced by microwave discharge. The emission spectra of most gases produced by RF or microwaves are similar to the emission spectrum produced by dc glow discharges [6]. An RF discharge utilizes either capacitive or inductive coupling. The high frequency electric field with capacitive coupling drives the discharge. In contrast, the time varying magnetic field with inductively coupling drives the discharge [9]. Usually, the continuous high frequency discharge generates the spectrum from the neutral atoms, although, at high power levels emission from singly ionized atoms might also occur. Increasing the power level and operating the high frequency oscillator intermittently, increases the light intensity due to the highly ionized atoms [6]. A typical plasma system consists of a vacuum chamber containing two parallel metal plates, which is a capacitor. One plate is typically ground and the other plate is connected to a 13.56 MHz RF power supply. The radio frequency field ionizes and then accelerates the free electrons, which in turn ionize other gas atoms, thereby generating secondary electrons. As the name suggests, secondary electrons arise from a collision with a free electron, as opposed to ionization due to the absorption of radiation by an atom. Secondary electrons generation also occurs when a charge particle with sufficient energy strikes the electrode. The initial bombarding electrons are primary electrons [10]. At high RF power levels, i.e. high electric fields, the rate of ionization produces an avalanche of electrons. The electron avalanche occurs because the mobile electrons in the plasma experience a strong acceleration via the high electric field, which increases the number of electron-atom scattering events and the energy transfer from the electron to the atom, which increases the rate of gas ionization. Due to the abundance of mobile electrons, the gas becomes electrically conductive. The interaction between the mobile electrons and atoms or molecules creates the plasma ignition. Due to the collisions, the atoms get excited and upon relaxation produces photons [11].

2.4 Helium Emission Lines

Scattering between electrons and the helium atoms in the plasma creates the line radiation that occurs via the electronic transition between energy levels in the He atoms and ions. The following example illustrates the reaction between an electron and a helium atom [9].

$$He + e\ (E1) \rightarrow He^* + e\ (E2)$$

On the left side of the reaction, the helium atom (He) is on the ground state. When the electron collides with the helium atom, it will excite the atom (He*) and move the electron that exists on the atomic orbital from the lower state (E1) to the higher state (E2), as shown on the right side of the reaction. The excited electron will decay back to its lower state (ground state), resulting in photon emission to conserve energy. The electron ground state of the helium atom is the subshell ($1s^2$). According to Pauli Exclusion Principle, the electrons must have opposite spins. They are designated by arrows that represent the electron spin quantum number. If the spin of the electron points up its spin quantum number of +1/2, while if it points down its spin quantum number is -1/2. In general, there is no excitation process if the energy of the electron is the same as the difference between the energy of the higher and lower state, since the electron would have to remain stable on its state after the interaction [9].

2.5 Helium Resonance lines of He I and He II

As mentioned in the previous section, the emission line spectrum occurs via the electronic transition between electron energy levels in the He atom. For He the two main emission lines are HeI and HeII. The Roman numbers refer to the line spectrum emitted from the neutral atom or emitted from ions of different degrees of ionization. For instance, the spectral emission from a neutral He atom is designated by He I. On the other hand, He II designated the spectral emission from a singly ionized He ion. In general, the shortest wavelengths emitted from a gas, be it He, Ne, etc., are generated from the highly ionized atoms. The shape of the radiation line, such as the width of the line and the sharpness of the line rely on the width of the energy levels in the transitions and rely on other conditions such as electric field, temperature and pressure. The transitions between excited states and the ground state of the atom or ions are the resonance lines. The first resonance line (the one that is generated from the lowest excited state to the ground state of the atom) is called raie ultime. For He II, the energy of the emitted photon is 40.81 eV or 303.781 A. The transition ($2p \rightarrow 1s$)

dominates the spectrum, which means that the electron relaxes from the lowest excited state (2p) to the ground state (1s). This is the transition of He II, which is known as the first resonance line and is emitted from the highly ionized atoms. When the transition (3p→1s) for He II is dictated by the spectrum, the electron transitions from the excited state (3p) to the ground state (1s), and it has a corresponding energy of 48.37 eV or a wavelength of 256.32 A [6]. Similarly, the He I has the raie ultime because it has the strongest transition line for its wavelength of 584.334 A or 21.22 eV (the first resonance line). The transition (2p→1s) is dominated by the spectrum and the electron emits from the excited state (2p) to the ground state (1s). The second resonance line for He I is given by the wavelength 537 A or 23.088 eV. The transition (3p→1s) is dominated the spectrum and the electron emits from the excited state (3p) to the ground state (1s). The He I radiation is dominated by the first resonance line of neutral helium. In general, the different discharge modes are important to generate the various excited species. So, either DC discharge or AC discharge are typically used to generate spectrum lines from neutral atoms or highly ionized atoms [6].

CHAPTER 3: Experimental Setup

3.1 The First effort is Microwave Spectroscopy

Apparatus

- Ion source works with high voltages and microwaves.

1. Leak valve for helium gas.
2. Resonator.
3. Microwave magnetron.
4. Quartz Capillary to confine the discharge in the capillary [6].
5. Cooling water.

- Differential vacuum pump: attached to the chamber to remove the gas molecules from the system and exhaust them to the atmosphere.
- Turbomolecular pump: attached to the main chamber that held Au target.
- Pressure Detector: to measure pressure inside plasma chamber.
- Power Supply**.**
- Collector mount on the top of the main chamber to measure the photocurrent. It is attached with a gold plate.
- Ammeter.

Microwave power is used to generate a gas plasma from which ions are extracted. The microwave generator consists of a microwave magnetron and operates at a frequency of 2.45 GHz. The output of the magnetron enters a resonant coupler or antenna that pumps the microwaves into a cylindrical microwave waveguide and on to a boron nitride He gas receptacle where the plasma forms.

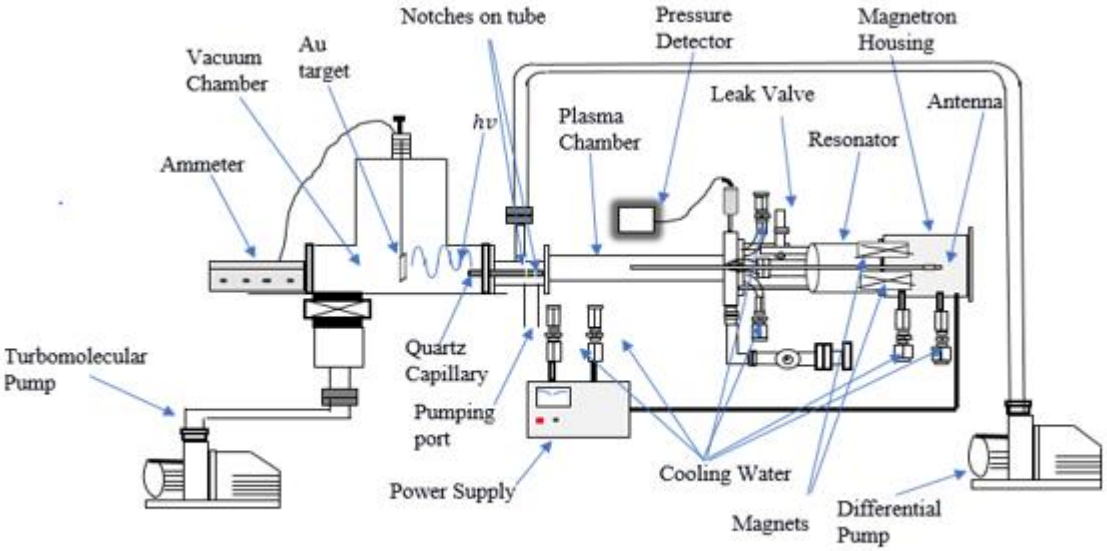

Figure 3.1 Microwave Schematic

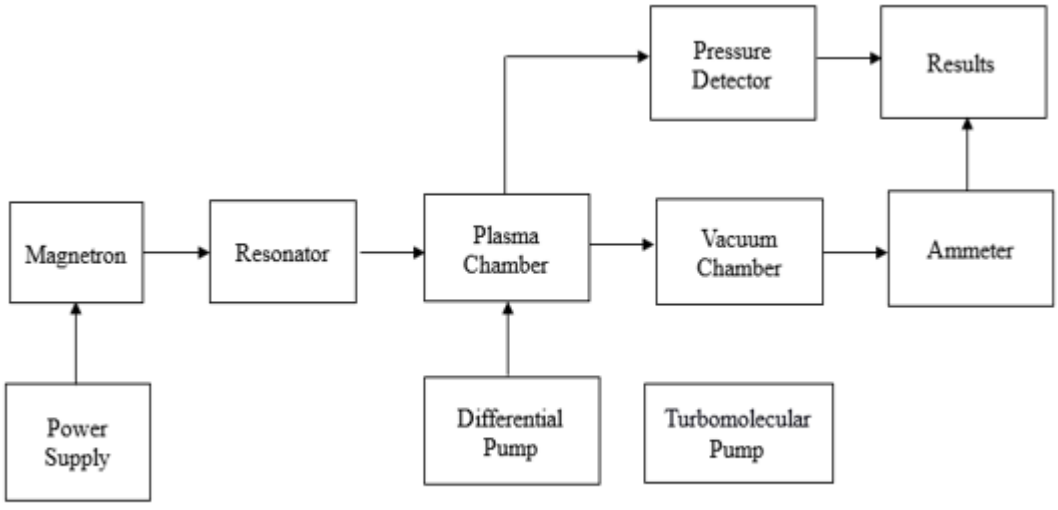

Figure 3.2 Block Diagram for Microwave System

Magnetic fields are oriented as in the following:

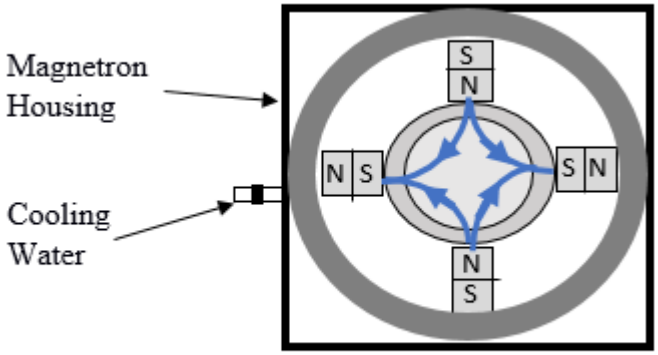

Figure 3.3 Magnetic Schematic

The microwaves generated in the source have to be delivered to the plasma chamber where the ECR occurs. This is done by using the coaxial cylinders as a waveguide (as explained in the Microwave manual). The cooling water is applied to the magnetron housing. The magnetron is used to provide microwaves for the plasma chamber. To generate microwaves a similar principle is at work as in electron cyclotron resonance. In the overall picture, an electric field is applied to the plasma in the magnetron, which accelerates the electrons. At the same time the magnetic field makes the electrons describe helixes on curved orbits. Charged particles in accelerated motion radiate electromagnetic waves. In the magnetron the waves are radiated at gyration frequency. As the electrons loose energy their gyration radius would be expected to decrease together with $v_{\perp}$, which would eventually remove the perpendicular component of motion. However, the electric field accelerates the electrons and therefore they sustain their velocities. In effect the magnetron converts the electric power into microwaves through sustaining the electric fields. The cooling water is described to be applied to the housing of the magnetron, which on the image would mean to the outside surface of the outer cylinder. The cylinders have to be coaxial to serve as a waveguide since the presence of symmetry allows for resonant frequencies in electromagnetic waves. The reason why two rather than one cylinder are necessary might be due to the design requirements needed for the waveguide or for confining the magnets.

Operation:

1. The system is pumped for 24 hours prior to operation in order to remove the gases inside the chamber.
1. Prior to igniting the plasma, open the cooling water valve. The cooling water keeps the unit from overheating and potential cracking the glass electrical feedthrough.
2. Prior to striking a plasma, open the leak valve to allow He to enter the plasma reactor to a pressure of approximately 40 mtorr.
3. Set the microwave power supply to 60 W and press the start button.

The plasma ignition happened after multiple efforts, but in some cases, it disappeared. Changing the cap inside the filament neutralizer and adjusting the distance of the antenna inside the microwave magnetron did not solve the ignition disappearance. In some cases, the plasma appeared in the viewpoint, but not through the chamber or the quartz tube. This was caused by overheating of the feedthrough, it indicated that the plasma was burning. According to the UV manual, if the plasma does not ignite, it suggests to turn off the magnetron and increase the gas flow rate. After we increased the magnetron power to 30 W, the plasma still disappeared. In the second effort, we used a different design for generating plasma, which is discussed in the next step.

3.2 Second effort with RF Plasma source:

Apparatus

Ion source: works with high voltages and RF Plasma.

1. Leak valve for helium gas.
2. Differential Pump.
3. Turbomolecular Pump.
4. Quartz Capillary.
5. Cooling water.
6. Matching Network (13.56 MHz) contains two capacitors in parallel and each is 500 PF and an inductive coil. It attaches in the end of the plasma Ion source.
7. Power Supply has forward power and reflected power. This generator attaches with two water cooling hoses.

8. Ammeter for measuring photocurrent.

Operation:

1. The system was typically pumped overnight before using the plasma source in order to remove the gases inside the chamber.
2. Open the water valve for cooling the system for 10 minutes prior to operation.
3. Open the leak valve in order to fill the chamber with helium gas. The helium gas pressure should be started from 30 mtorr or higher.
4. Operate the power at an appropriate value, usually we started with 60 W.
5. Press power on.

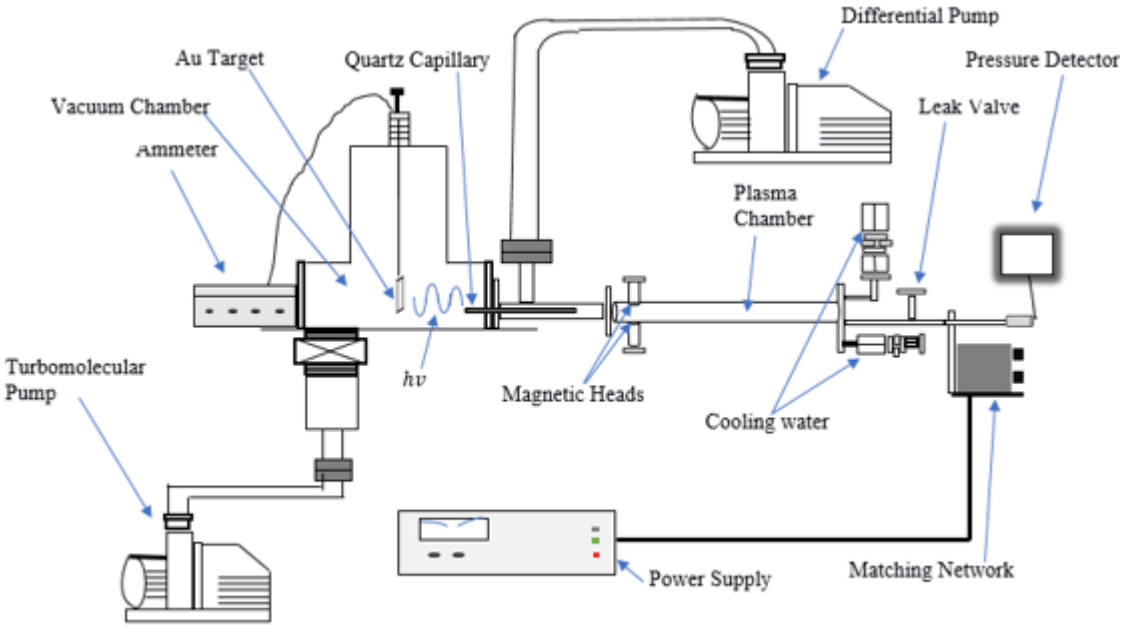

Figure 3.4 RF Schematic

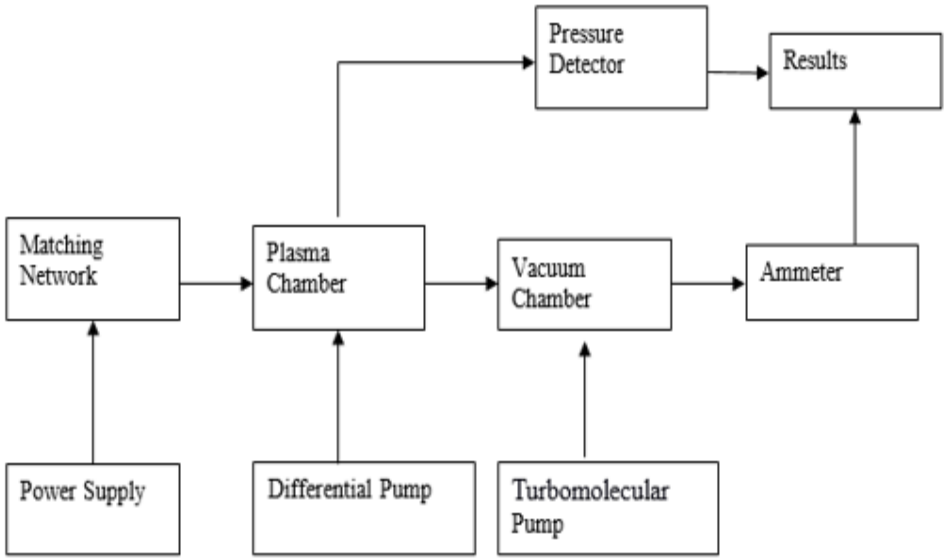

Figure 3.5 Block Diagram for RF system

Experimental Effort:

We started the experiment after pumping the chamber one day before the experiment. After doing all setups of the experiment the plasma did not ignite. Increasing the power and trying to tune the matching network did not contribute to pushing the reflected power to 0 watts. After several efforts, we used the capacitors that have 33 pF and 50 pF in series in order to fix the reflected power. The matching network with impedance at 50 Ohm load was used to transfer the radio frequency power inside the chamber. In our case, the reflected power did not go to zero for some reason, despite adjusting the tune of the matching box. In turn, the power reflected to the generator was high, which made it overheat.

3.3 The Third Effort:

Capacitive RF Plasma Source:

Apparatus: (See figures 3.6 and 3.9)

1. Plasma Chamber (stainless steel tube).
2. Matching Network.
3. Leak Valve.
4. Quartz Tube.

5. Power Supply.
6. Two Vacuum Pumps.
7. Cooling Valves.
8. Copper Rod.
9. Magnet Heads.
10. Ammeter.

Experimental design

The chamber design is a stainless steel tube which is attached to the vacuum chamber. The leak valve for introducing helium gas is mounted on the stainless steel tube. The leak valve allows precise control of the He gas pressure in the UV. The turbomolecular pump is attached to the main chamber that contains the detector of the photocurrent on the top of the main chamber. The pressure of the main chamber should be around 1×10^{-6} mtorr. Another mechanical pump is connected to the stainless steel tube to remove gas and molecules inside the plasma chamber. The pressure of the stainless steel should be around 1×10^{-6} mtorr and the turbomolecular pump operates at 1500 Hz or rpm. The copper rod with 51 cm is constructed inside the stainless steel cavity. It has a hole in the end of the rod in order to attach the matching network on it, which is called a cathode. The plasma will transmit inside the hole of the copper rod. The magnetic heads are inserted inside the stainless steel and the heads are covered by the molybdenum foil. The copper coil is rolled around the magnetic heads and is provided with cooling water in order to keep the surface of the plasma chamber cold. The end of the copper rod is a disk shape with another constructed disk shape in front of it 1.5” away in order to be parallel with the plate electrodes. The other disk has a hole in the center in order to put the quartz tube through the hole. The plasma is produced between two disk-shaped electrodes that are constructed parallel to each other inside the chamber.

For this design, we used the matching network with impedance at 50 Ohm load. The matching network has an inductive coil and two capacitors with 500 PF for each. We started with 33 PF capacitors in series in order to reflect the power inside the chamber by using the tune switch in the matching box. However, the power did not go to zero watts, causing the power supply to overheat. The capacitor at 50 PF gives the previous result, which makes the

power reverse to the power supply and causes the generator to overheat. Reducing the number of coil turns by attaching copper on the coils did not solve the power reflection. Solving this problem required changing the matching network to pi network (see figure 3.9) which consists of capacitors and an inductor. The matching unit with two capacitors was appropriate for our experiment and led the reflection power to lie at zero after adjusting the switching tune. In this case, the power transferred into the chamber to produce plasma.

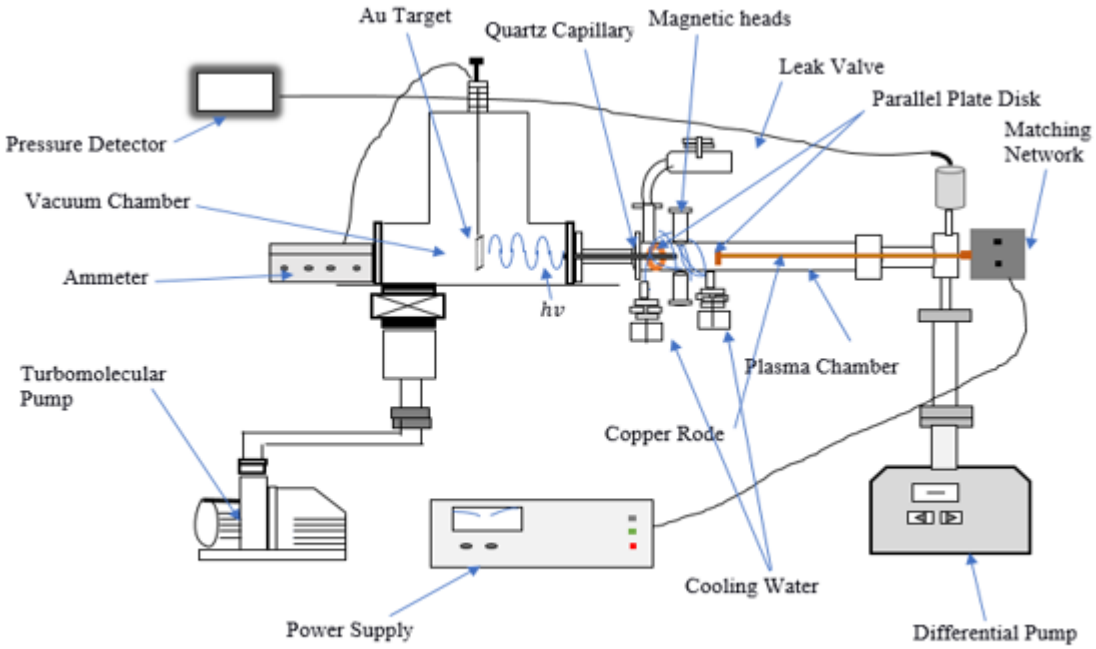

Figure 3.6 RF Schematic

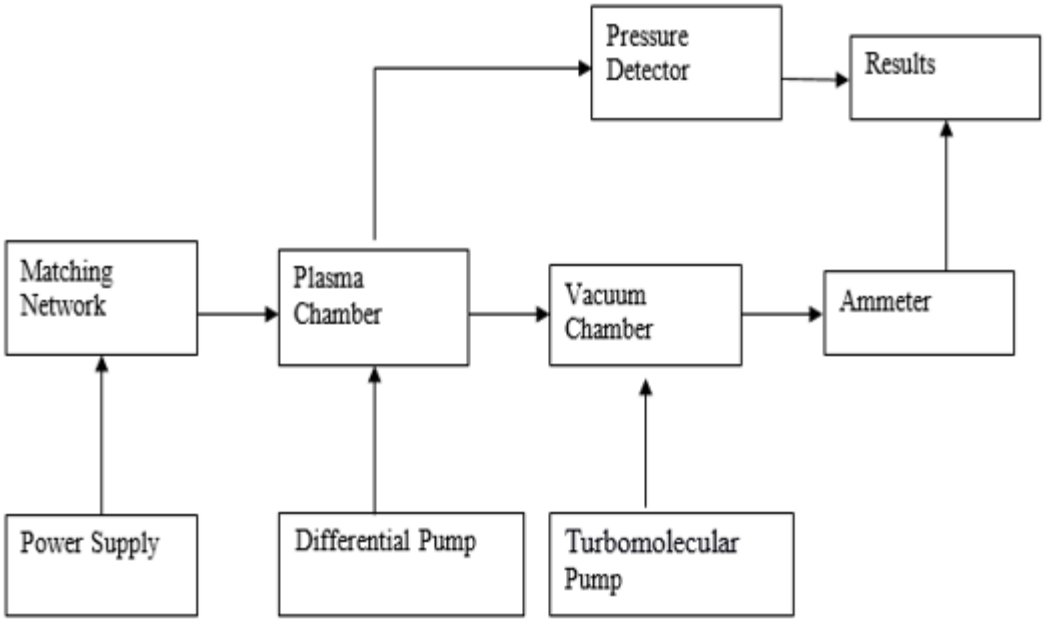

Figure 3.7 Block Diagram for RF System

In our experiment, the magnets should be oriented as in the following diagram:

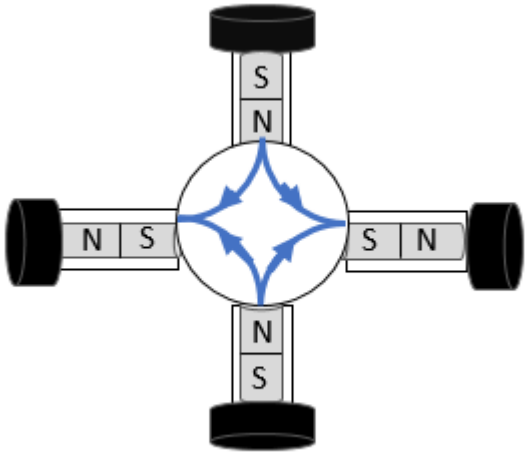

Figure 3.8 Magnetic Heads

The orientation ensures that the structure of the magnetic field is quadrupolar. This is useful in order to confine the plasma to the inner regions of the plasma chamber.

3.4. Method for Data Acquisition

Set up:

1. Open 4 cooling valves.

2. Wait about 10 minutes until the power supply and the chamber surface becomes cold.
3. Open Helium gas and increase it until 30 mtorr in order to get the first plasma ignition.
4. Run the power supply and set the forward power at 10 W.
5. Now, change the power to reverse power in order to reflect the power inside the chamber. Note that the reverse power should go to zero watts by using the tune in the matching unit.
6. After the above steps the plasma ignites and it is possible to see the plasma from the mirror.
7. The photon strikes the gold surface and the photoelectrons will go to the detector to measure how much photocurrent is produced.
8. Repeat the steps (4) and (5) by increasing the forward power and tune the reverse power to zero by using the matching unit tunes.

The photocurrent was collected multiple times at each He pressure and plasma power. The data sets for a specific He pressure and plasma power were then averaged. The objective of taking the average of photocurrent was to achieve the accurate magnitude for the photocurrent (See Table 1). In order to ignite the plasma, the gas pressure needed to be greater than 30 mtorr, as this made it possible to decrease the helium pressure gradually without losing the ignition. The goal was to collect the data and plot the curve for the average of photocurrent versus the power at specific pressures. The curve shows that the highest value for the average photocurrent is at the pressure of 60 mtorr. It also shows that there is no photocurrent below 2.34 mtorr (See figure 4.1, in chapter 4).

The second objective was to plot the photocurrent as a function of helium pressure. Data was collected per power setting from 10 W to 100 W at a given pressure. For example, at 10 W and 2.34 mtorr of He pressure the average of the photocurrent was 1.150 pA. At 10 W and 3.24 mtorr of He pressure the average of photocurrent was 1.075 pA. This enabled the data to be plotted so that the He I and He II peaks could be observed and qualitatively evaluate their intensities (See Table 2 in the Appendix). This enabled the data to be ploted so that the He I and He II peaks could be observed and qualitatively evaluate their intensities (See Table 2 in the Appendix).

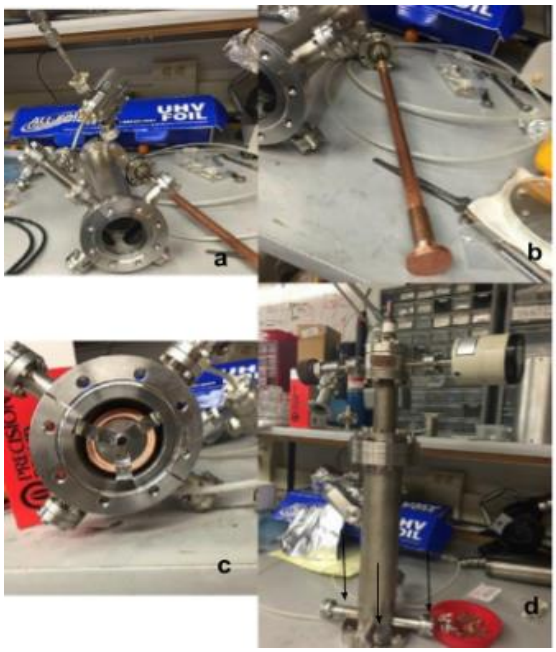

a) Plasma chamber.
b) The copper rod.
c) Desk.
d) Plasma chamber includes magnetic heads, pumping ports and leak valve.

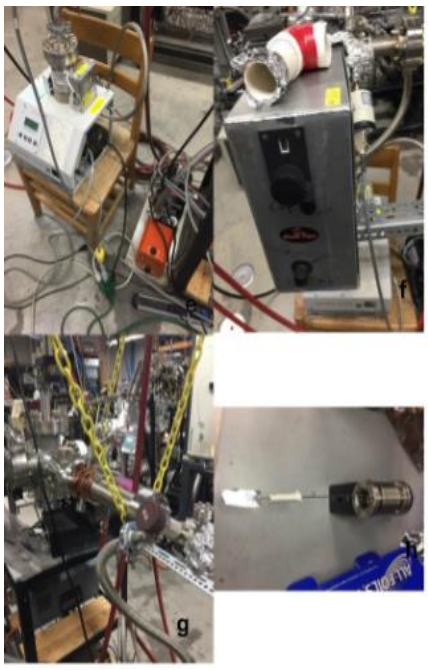

e) Two mechanical pumps.
f) Matching Network.
g) The plasma chamber with cooling system.
h) Gold Substrate.

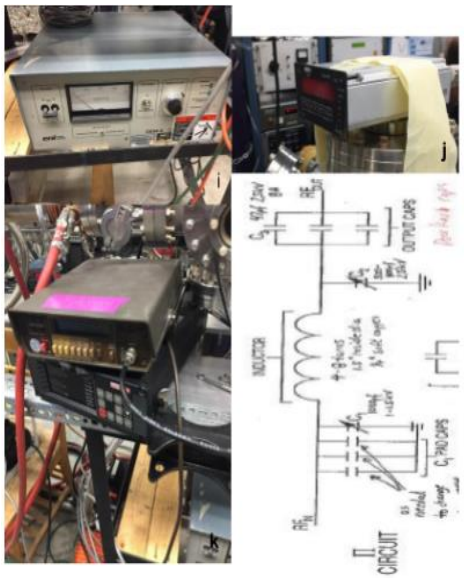

i) Power Supply.
j) Pressure Detector.
k) Ammeter.
l) PI Circuit.

Figure 3.9 Experimental Design for RF Setup

CHAPTER 4: Results

Data and Results

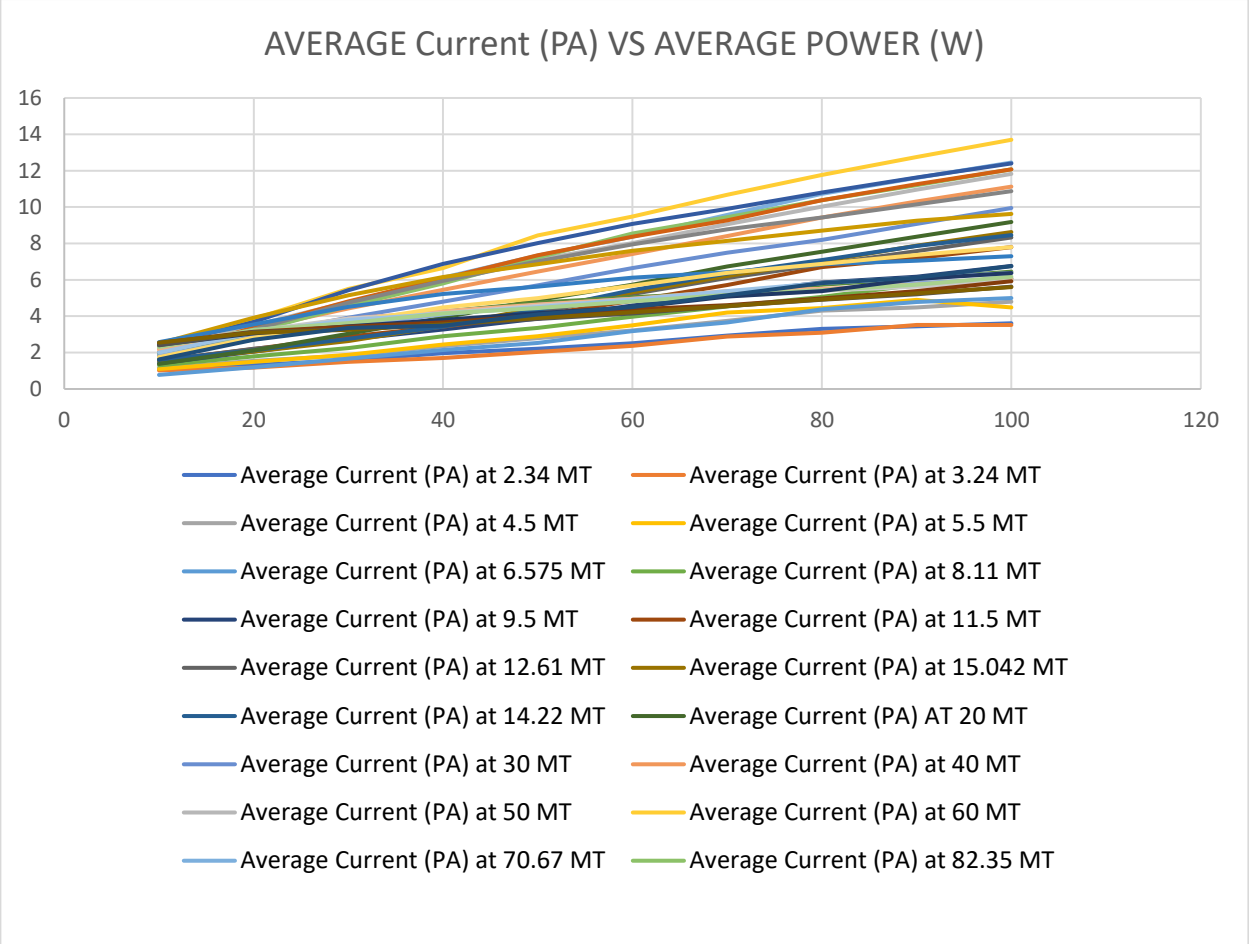

The Figure 4.1. The average power and the average of photocurrent at specific pressures. It shows how much photocurrent is produced in the function of power. The first step is to make plot the photocurrent at specific magnitude of power and pressure. The pressure 60 mtorr shows the highest value of photocurrent. The graph shows that below the pressure 2.34 mtorr, there is no plasma ignition, which means no photocurrent is produced.

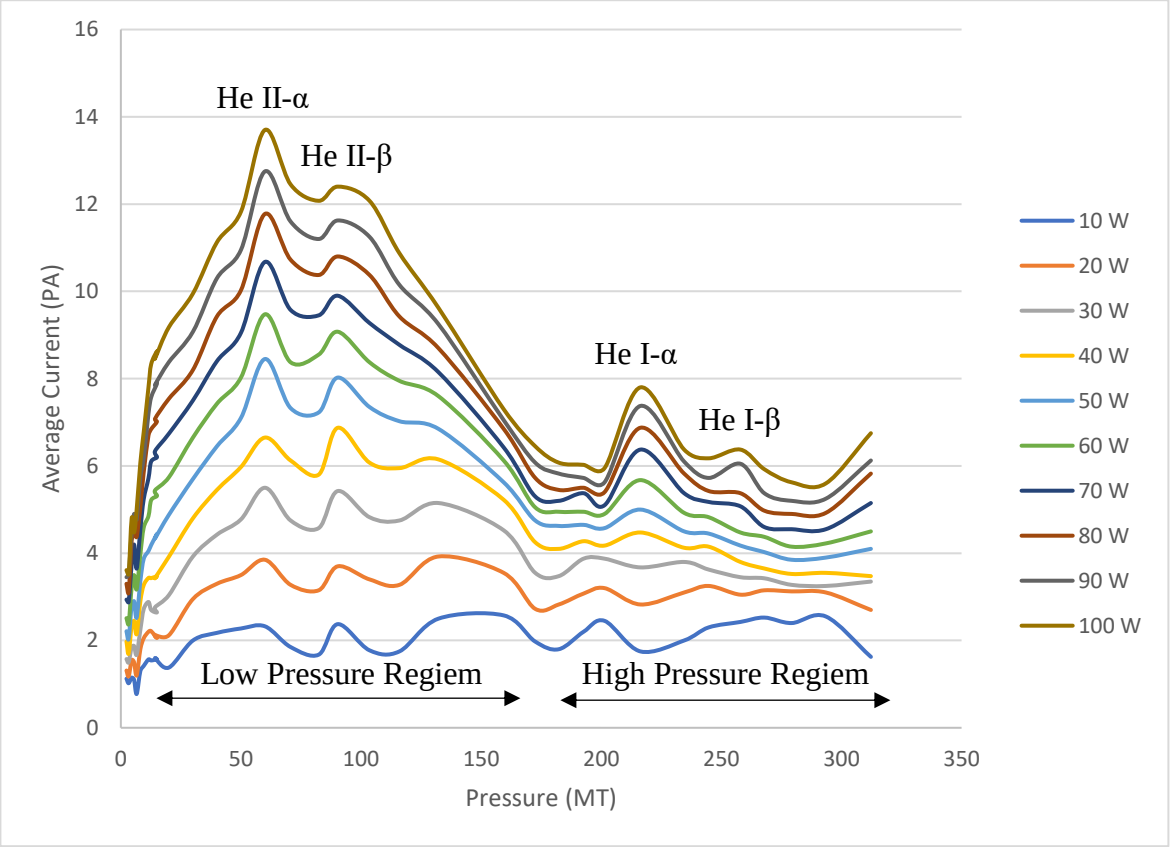

Figure 4.2 The average photocurrent for every magnitude of power and pressure. It is the desire plot for our data. It shows the two peaks in the operation of the helium gas at low pressure and two peaks at high pressure.

CHAPTER 5: Discussion

We have used radio frequency power to excite helium gas and indirectly analyzed the helium emission resonance lines and photon energies at varies pressure. This evaluation occurs by measuring the average current of gold substrate placed in the beam of the light source. We have measured the average current on the order a few picoamps, as opposed to nanoamps for traditional DC helium plasmas. The strength of magnetic field and their position in plasma system can produce maximum UV light and then high photocurrent. Increasing the cross section of magnetic field would increase the number of collision in plasma. We are measuring the photocurrent in the order of few pA, because the strength of magnetic field is not high enough to generate high flux of UV light and photocurrent in the order of nA. The intensity of ultraviolet emission has been achieved by increasing the pumping of helium gas and radio frequency power. In addition, the ECR technique was incorporated into the apparatus to raise the probability of collision between free electrons and helium gas, resulting in higher intensity emission of ultraviolet light. Generally, the heated electrons collide with plasma particles, ionize them and therefore impart energy to the plasma through collisions. The profile of the photocurrent (average current) consists of helium II and helium I peaks at low and high pressure regimes, respectively, where the literature has indicated that the emission of the helium resonance lines for helium II and helium I peaks are pressure dependent [6,14-19].

The first peak in Fig. 4.2 at low helium gas pressure is assigned to the helium II-α resonance emission line with a corresponding energy of 40.8 eV and the second peak to the helium II- β resonance emission line with corresponding energy of 48.3 eV. The pair maxima of helium II resonance emission line at low pressure are specifically the Lyman-alpha (40.8 eV at 30.38 nm) and Lyman-beta (48.3 eV at 25.6 nm), respectively. The transition from state (2p) to state (1s) is considered as Lyman-alpha, while the transition from state (3p) to state (1s) is Lyman-beta [6]. In fact, the Lyman-alpha peak has the highest photocurrent while the Lyman-beta peak generates a lower photocurrent. This was proposed by Mills, R., & Ray, P. [13], when they observe the helium II peaks at wavelength 30.38 nm and 25.6 nm. Their data show that the peak at 30.38 nm has a higher photon count rate than the peak at 25.6 nm.

In high He pressure region in Fig. 4.2, the helium II gets quenched due to interactions with other helium atoms. At high power and high gas pressure, the inelastic collision between electrons and helium atoms produces photon with energies of 21.2 eV and 23.1 eV. It is hypothesized that the pair maxima of helium I resonance emission line at high pressure region are assigned to Lyman-alpha (21.2 eV at 58.48 nm), and Lyman-beta (23.1 eV at 53.67 nm), respectively. According to Samson, helium I-alpha at 21.1 eV has a higher photon count rate than helium I-beta at 23.1 eV. This agrees with our data, where we have identified the peak corresponding to a higher photocurrent to the helium I-alpha and the less intense peak to the helium I-beta. The helium I emission occurs when there is a transition from the energy state (2p) to the energy state (1s) with the wavelength 58.48 nm. Also, the transition from the energy state (3p) to the energy state (1s) with the wavelength 53.67 nm is known as Lyman-beta [14].

CHAPTER 6: Conclusion

We have reported on the design and operation of a RF powered helium gas discharge ultraviolet light source. The pressure depending photocurrent of the RF helium UV light source is summarized in Fig. 4.2. It clearly demonstrates the pressure dependence of the photocurrent (UV light emission) at low and high He pressure. We have concluded that the incorporation of ECR in an RF plasma increases the intensity of UV light emission by increasing the probability of collisions and the subsequent generation of excited states of He. The first two peaks in the low pressure region correspond to photon energies of 40.8 eV and 48.3 eV and the latter peaks in the high pressure region correspond to photon energies of 21.2 eV and 23.1 eV. According to Samson [6], at low He pressure the emission is due to helium II excited state, where the first peak is the first resonance line of transition from the 2p to the 1s state, with a corresponding a photon energy of 40.8 eV. The second peak is the second resonance line of the transition from the 3p to the 1s state, with a corresponding photon energy of 48.3 eV. In the high pressure region, the emission is due to the helium I excited state, where the first peak is the first resonance line of the transition from the 2p to the 1s state, with a corresponding photon energy of 21.2 eV. The second peak in the high pressure region is the transition from the 3p to the 1s state, with a corresponding photon energy of 23.1 eV [6,14]. The first resonance lines for helium I and helium II correspond to Lyman alpha transitions, while the second resonance lines correspond to Lyman beta transitions [6,14].

6.1. Future Work:

It is clear that more work is needed to increase the photocurrent from the pA to nA range. We were unable to visualize the effect of ECR on the plasma. Consequently, the strength of the magnets and their position relative to the center of the plasma isn’t optimal, where optimization is defined as maximum UV light emission through the quartz capillary. Note, for full advantage of ECR, one wants the electrons trapped in the magnetic field centered on the axis of the capillary tube and that the radius of their circular trajectory is less than the radius of the capillary. In defense of our experimental strategy, we were primarily interested in demonstrating that an integrated RF/ECR plasma could generate UV light. Therefore, optimizing the electron trap and ECR confined plasma is the next step in the evolution of the UV light source.

Reference

[1] Serway, R. A., & Jewett, J. W. (2008). *Physics for scientists and engineers with modern physics* (7th ed.). Australia: Thomson/Brooks/Cole.

[2] Serway, R. A., Moses, C. J., & Moyer, C. A. (2005). *Modern physics* (3rd ed.). Belmont, CA: Thomson Brooks/Cole.

[3] Tipler, P. A., Llewellyn, R. A., & Llewellyn, M. J. (2012). *Modern physics* (6th ed.). New York: W. H. Freeman and Co.

[4] Thornton, S. T., & Rex, A. F. (2013). *Modern physics for scientists and engineers* (4th ed.). Boston, MA: Cengage Learning.

[5] Yang, F., & Hamilton, J. H. (2010). *Modern atomic and nuclear physics* (Revised ed.). New Jersey: World Scientific.

[6] Samson J. A. R. (1961). *Techniques of Vacuum Ultraviolet Spectroscopy* (New York: Wiley).

[7] Hakanson, J. B., Meeks, W., & Rovey, J. L. Plasma Theory for Undergraduate Education.

[8] Lieberman, M. A., & Lichtenberg, A. J. (1994). *Principles of plasma discharge for materials processing* (1st ed.). New York: John Wiley & Sons.

[9] Boulos, M. I., Fauchais, P., & Pfender, E. (1994). *Thermal plasmas* (1994 ed.). New York: Plenum Press.

[10] Bruining, H. (1962). *Physics and Applications of Secondary Electron Emission: Pergamon Science Series: Electronics and Waves—a Series of Monographs*. Elsevier.

[11] Knoll, G. F. (2000). *Radiation detection and measurement*. John Wiley & Sons.

[12] Budtz-Jørgensen, C. V. (2001). *Studies of Electrical Plasma Discharges* (Doctoral dissertation, thèse de doctorat de l'Université Aarhus, Danemark).

[13] Mills, R., & Ray, P. (2003). Extreme ultraviolet spectroscopy of helium–hydrogen plasma. *Journal of Physics D: Applied Physics*, *36*(13), 1535.

[14] Damany, N., Romand, J., & Vodar, B. (Eds.). (1974). *Some Aspects of Vacuum Ultraviolet Radiation Physics: International Series of Monographs in Natural Philosophy* (Vol. 66). Elsevier.

[15] Gengeliczki, Z. (2008). *Electronic structure and gas phase thermochemistry of organoelement and organometallic compounds* (Doctoral dissertation, INSTITUTE OF CHEMISTRY BUDAPEST).

[16] Neupane, M. (2010). *Angle-Resolved Photoemission Studies on Ruthenates and Iron-Based Superconductors*. Boston College.

[17] Schonhense, G., & Heinzmann, U. (1983). A capillary discharge tube for the production of intense VUV resonance radiation. *Journal of Physics E: Scientific Instruments*, *16*(1), 74.

[18] Collins, C. B., & Robertson, W. W. (1964). Helium Afterglow. I. Atomic Spectrum. *The Journal of Chemical Physics*, *40*(8), 2202-2208.

[19] Collins, C. B., & Robertson, W. W. (1964). Helium Afterglow. II. Molecular Spectrum. *The Journal of Chemical Physics*, *40*(8), 2208-2211.

[20] Goldston, R. J., & Rutherford, P. H. (1995). *Introduction to plasma physics*. CRC Press.

[21] Eliezer, S., & Eliezer, Y. (2001). *The fourth state of matter: an introduction to plasma science*. CRC Press.

[22] Inan, U. S., & Gołkowski, M. (2010). *Principles of plasma physics for engineers and scientists*. Cambridge University Press.

[23] Hassouba, M. A., & Dawood, N. (2014). A Comparative Spectroscopic Study on Emission Characteristics of DC and RF Discharges Plasma using Different Gases. *Life Science Journal*, *11*(9).

[24] Giordano, N. (2013). *College physics: reasoning and relationships*. Boston, MA: Cengage Learning.

[25] Naidu, M. S. (2013). *High voltage engineering*. Tata McGraw-Hill Education.

[26] Myers, R. L. (2006). *The basics of physics*. Greenwood Publishing Group.

[27] Tarvainen, O. (2005). Studies of electron cyclotron resonance ion source plasma physics. *Research report/Department of Physics, University of Jyväskylä no. 8/2005.*

Appendix

Table 1.

Average Power (W)	Average Current (PA) at 2.34 MT	Average Current (PA) at 3.24 MT	Average Current (PA) at 4.5 MT	Average Current (PA) at 5.5 MT	Average Current (PA) at 6.575 MT	Average Current (PA) at 8.11 MT	Average Current (PA) at 9.5 MT	Average Current (PA) at 11.5 MT
10	1.150	1.075	1.150	1.100	0.775	1.450	1.325	1.475
20	1.325	1.225	1.550	1.500	1.200	1.800	2.275	2.100
30	1.575	1.550	1.850	1.875	1.675	2.350	2.575	2.775
40	2.025	1.725	2.350	2.450	2.150	2.875	3.500	3.275
50	2.275	2.050	2.800	2.900	2.525	3.525	3.800	3.925
60	2.625	2.375	3.225	3.500	3.175	3.925	4.675	4.475
70	3.025	2.900	3.750	4.200	3.650	4.550	5.300	5.425
80	3.375	2.975	4.300	4.450	4.375	5.075	5.750	6.500
90	3.475	3.550	4.475	4.900	4.775	5.825	6.150	6.975
100	3.575	3.400	4.800	4.475	5.000	5.750	6.750	7.550

Average Power (W)	Average Current (PA) at 12.61 MT	Average Current (PA) at 15.042 MT	Average Current (PA) at 14.22 MT	Average Current (PA) AT 20 MT	Average Current (PA) at 30 MT	Average Current (PA) at 40 MT	Average Current (PA) at 50 MT	Average Current (PA) at 60 MT
10	1.650	1.700	1.800	1.350	2.000	2.175	2.275	2.325
20	2.225	2.175	2.400	2.100	2.950	3.300	3.500	3.850
30	2.650	2.875	3.050	2.975	3.925	4.425	4.775	5.500
40	3.425	3.550	3.800	3.900	4.800	5.450	5.975	6.650
50	4.275	4.650	4.900	4.900	5.700	6.450	7.100	8.450
60	5.150	5.575	5.925	5.775	6.650	7.425	8.025	9.475
70	6.125	6.500	6.750	6.800	7.500	8.400	9.050	10.675
80	6.850	7.325	7.500	7.625	8.200	9.425	10.025	11.775
90	7.675	8.275	8.225	8.475	9.075	10.300	10.950	12.750
100	8.400	9.000	8.750	9.350	9.950	11.125	11.825	13.700

Average Power (W)	Average Current (PA) at 70.67 MT	Average Current (PA) at 82.35 MT	Average Current (PA) at 90.325 MT	Average Current (PA) at 103.52 MT	Average Current (PA) at 115.95 MT	Average Current (PA) at 132.2 MT	Average Current (PA) at 159.37 MT	Average Current (PA) at 172.5 MT
10	1.850	1.675	2.375	1.775	1.750	2.500	2.575	1.975
20	3.275	3.150	3.700	3.400	3.275	3.925	3.550	2.725
30	4.750	4.575	5.425	4.825	4.750	5.150	4.525	3.550
40	6.125	5.800	6.875	6.075	5.950	6.150	5.225	4.250
50	7.325	7.225	8.025	7.350	7.025	6.850	5.625	4.750
60	8.375	8.550	9.075	8.375	7.950	7.600	6.125	5.050
70	9.575	9.450	9.900	9.275	8.775	8.150	6.425	5.300
80	10.725	10.375	10.800	10.375	9.425	8.700	6.850	5.725
90	11.600	11.200	11.625	11.250	10.150	9.250	7.050	6.075
100	12.450	12.075	12.400	12.075	10.875	9.625	7.300	6.450

Average Power (W)	Average Current (PA) at 182.3 MT	Average Current (PA) at 192.62 MT	Average Current (PA) at 201.37 MT	Average Current (PA) at 216.3 MT	Average Current (PA) at 234.5 MT	Average Current (PA) at 244.72 MT	Average Current (PA) at 257.92 MT	Average Current (PA) at 267.87 MT
10	1.800	2.200	2.450	1.750	2.000	2.300	2.425	2.525
20	2.825	3.075	3.200	2.825	3.100	3.250	3.050	3.150
30	3.475	3.875	3.875	3.675	3.800	3.625	3.450	3.425
40	4.100	4.275	4.175	4.475	4.125	4.150	3.800	3.650
50	4.625	4.650	4.575	5.000	4.500	4.450	4.175	4.025
60	4.950	4.950	4.900	5.675	4.925	4.825	4.475	4.375
70	5.200	5.375	5.100	6.375	5.375	5.175	5.075	4.600
80	5.450	5.500	5.400	6.875	5.825	5.425	5.375	4.975
90	5.825	5.725	5.625	7.375	6.100	5.725	6.050	5.375
100	6.075	6.025	5.950	7.800	6.375	6.175	6.375	5.925

Average Power (W)	Average Current (PA) at 279.25 MT	Average Current (PA) at 293.5 MT	Average Current (PA) at 312.25 MT
10	2.400	2.550	1.625
20	3.125	3.100	2.700
30	3.275	3.250	3.350
40	3.525	3.550	3.475
50	3.850	3.900	4.100
60	4.150	4.225	4.500
70	4.550	4.550	5.150
80	4.900	4.925	5.825
90	5.200	5.250	6.125
100	5.625	5.600	6.750

Table 2.

Power (W)	Pressure (MT)	Average Current (PA)	Pressure (MT)	Average Current (PA)
10	2.34	1.150	90.325	2.375
	3.24	1.075	103.52	1.775
	4.5	1.150	115.95	1.750
	5.5	1.100	132.2	2.500
	6.575	0.775	159.37	2.575
	8.11	1.450	172.5	1.975
	9.5	1.325	182.3	1.800
	11.5	1.475	192.62	2.200
	12.61	1.650	201.37	2.450
	15.042	1.700	216.3	1.750
	14.22	1.800	234.5	2.000
	20	1.350	244.72	2.300
	30	2.000	257.92	2.425
	40	2.175	267.87	2.525
	50	2.275	279.25	2.400
	60	2.325	293.5	2.550
	70.67	1.850	312.25	1.625
	82.35	1.675		

Power (W)	Pressure (MT)	Average Current (PA)	Pressure (MT)	Average Current (PA)
20	2.34	1.325	90.325	3.700
	3.24	1.225	103.52	3.400
	4.5	1.550	115.95	3.275
	5.5	1.500	132.2	3.925
	6.575	1.200	159.37	3.550
	8.11	1.800	172.5	2.725
	9.5	2.275	182.3	2.825
	11.5	2.100	192.62	3.075
	12.61	2.225	201.37	3.200
	15.042	2.175	216.3	2.825
	14.22	2.400	234.5	3.100
	20	2.100	244.72	3.250
	30	2.950	257.92	3.050
	40	3.300	267.87	3.150
	50	3.500	279.25	3.125
	60	3.850	293.5	3.100
	70.67	3.275	312.25	2.700
	82.35	3.150		

Power (W)	Pressure (MT)	Average Current (PA)	Pressure (MT)	Average Current (PA)
30	2.34	1.575	90.325	5.425
	3.24	1.550	103.52	4.825
	4.5	1.850	115.95	4.750
	5.5	1.875	132.2	5.150
	6.575	1.675	159.37	4.525
	8.11	2.350	172.5	3.550
	9.5	2.575	182.3	3.475
	11.5	2.775	192.62	3.875
	12.61	2.650	201.37	3.875
	15.042	2.875	216.3	3.675
	14.22	3.050	234.5	3.800
	20	2.975	244.72	3.625
	30	3.925	257.92	3.450
	40	4.425	267.87	3.425
	50	4.775	279.25	3.275
	60	5.500	293.5	3.250
	70.67	4.750	312.25	3.350
	82.35	4.575		

Power (W)	Pressure (MT)	Average Current (PA)	Pressure (MT)	Average Current (PA)
40	2.34	2.025	90.325	6.875
	3.24	1.725	103.52	6.075
	4.5	2.350	115.95	5.950
	5.5	2.450	132.2	6.150
	6.575	2.150	159.37	5.225
	8.11	2.875	172.5	4.250
	9.5	3.500	182.3	4.100
	11.5	3.275	192.62	4.275
	12.61	3.425	201.37	4.175
	15.042	3.550	216.3	4.475
	14.22	3.800	234.5	4.125
	20	3.900	244.72	4.150
	30	4.800	257.92	3.800
	40	5.450	267.87	3.650
	50	5.975	279.25	3.525
	60	6.650	293.5	3.550
	70.67	6.125	312.25	3.475
	82.35	5.800		

Power (W)	Pressure (MT)	Average Current (PA)	Pressure (MT)	Average Current (PA)
50	2.34	2.275	90.325	8.025
	50	2.050	103.52	7.350
	4.5	2.800	115.95	7.025
	5.5	2.900	132.2	6.850
	6.575	2.525	159.37	5.625
	8.11	3.525	172.5	4.750
	9.5	3.800	182.3	4.625
	11.5	3.925	192.62	4.650
	12.61	4.275	201.37	4.575
	15.042	4.650	216.3	5.000
	14.22	4.900	234.5	4.500
	20	4.900	244.72	4.450
	30	5.700	257.92	4.175
	40	6.450	267.87	4.025
	50	7.100	279.25	3.850
	60	8.450	293.5	3.900
	70.67	7.325	312.25	4.100
	82.35	7.225		

Power (W)	Pressure (MT)	Average Current (PA)	Pressure (MT)	Average Current (PA)
60	2.34	2.625	90.325	9.075
	3.24	2.375	103.52	8.375
	4.5	3.225	115.95	7.950
	5.5	3.500	132.2	7.600
	6.575	3.175	159.37	6.125
	8.11	3.925	172.5	5.050
	9.5	4.675	182.3	4.950
	11.5	4.475	192.62	4.950
	12.61	5.150	201.37	4.900
	15.042	5.575	216.3	5.675
	14.22	5.925	234.5	4.925
	20	5.775	244.72	4.825
	30	6.650	257.92	4.475
	40	7.425	267.87	4.375
	50	8.025	279.25	4.150
	60	9.475	293.5	4.225
	70.67	8.375	312.25	4.500
	82.35	8.550		

Power (W)	Pressure (MT)	Average Current (PA)	Pressure (MT)	Average Current (PA)
70	2.34	3.025	90.325	9.900
	3.24	2.900	103.52	9.275
	4.5	3.750	115.95	8.775
	5.5	4.200	132.2	8.150
	6.575	3.650	159.37	6.425
	8.11	4.550	172.5	5.300
	9.5	5.300	182.3	5.200
	11.5	5.425	192.62	5.375
	12.61	6.125	201.37	5.100
	15.042	6.500	216.3	6.375
	14.22	6.750	234.5	5.375
	20	6.800	244.72	5.175
	30	7.500	257.92	5.075
	40	8.400	267.87	4.600
	50	9.050	279.25	4.550
	60	10.675	293.5	4.550
	70.67	9.575	312.25	5.150
	82.35	9.450		

Power (W)	Pressure (MT)	Average Current (PA)	Pressure (MT)	Average Current (PA)
80	2.34	3.375	90.325	10.800
	3.24	2.975	103.52	10.375
	4.5	4.300	115.95	9.425
	5.5	4.450	132.2	8.700
	6.575	4.375	159.37	6.850
	8.11	5.075	172.5	5.725
	9.5	5.750	182.3	5.450
	11.5	6.500	192.62	5.500
	12.61	6.850	201.37	5.400
	15.042	7.325	216.3	6.875
	14.22	7.500	234.5	5.825
	20	7.625	244.72	5.425
	30	8.200	257.92	5.375
	40	9.425	267.87	4.975
	50	10.025	279.25	4.900
	60	11.775	293.5	4.925
	70.67	10.725	312.25	5.825
	82.35	10.375		

Power (W)	Pressure (MT)	Average Current (PA)	Pressure (MT)	Average Current (PA)
90	2.34	3.475	90.325	11.625
	3.24	3.550	103.52	11.250
	4.5	4.475	115.95	10.150
	5.5	4.900	132.2	9.250
	6.575	4.775	159.37	7.050
	8.11	5.825	172.5	6.075
	9.5	6.150	182.3	5.825
	11.5	6.975	192.62	5.725
	12.61	7.675	201.37	5.625
	15.042	8.275	216.3	7.375
	14.22	8.225	234.5	6.100
	20	8.475	244.72	5.725
	30	9.075	257.92	6.050
	40	10.300	267.87	5.375
	50	10.950	279.25	5.200
	60	12.750	293.5	5.250
	70.67	11.600	312.25	6.125
	82.35	11.200		

Power (W)	Pressure (MT)	Average Current (PA)	Pressure (MT)	Average Current (PA)
100	2.34	3.575	90.325	12.400
	3.24	3.400	103.52	12.075
	4.5	4.800	115.95	10.875
	5.5	4.475	132.2	9.625
	6.575	5.00	159.37	7.300
	8.11	5.750	172.5	6.450
	9.5	6.750	182.3	6.075
	11.5	7.550	192.62	6.025
	12.61	8.400	201.37	5.950
	15.042	9.00	216.3	7.800
	14.22	8.750	234.5	6.375
	20	9.350	244.72	6.175
	30	9.950	257.92	6.375
	40	11.125	267.87	5.925
	50	11.825	279.25	5.625
	60	13.700	293.5	5.600
	70.67	12.450	312.25	6.750
	82.35	12.075		